ARTICLE

Mononuclear Carbonyl Anion Complexes of Groups IV and V Metals

Shu-jun Lei, Yang-yu Zhou, Xiao-yang Jin, Guan-jun Wang*, Ming-fei Zhou*

Collaborative Innovation Center of Chemistry for Energy Materials, Department of Chemistry, Shanghai Key Laboratory of Molecular Catalysis and Innovative Materials, Fudan University, Shanghai 200438, China

(Dated: Received on May 25, 2021; Accepted on July 8, 2021)

The anionic carbonyl complexes of groups IV and V metals $TM(CO)_{6,7}$ (TM=Ti, Zr, Hf, V, Nb, Ta) are prepared in the gas phase using a laser vaporation-supersonic expansion ion source. The infrared spectra of $TM(CO)_{6,7}^-$ anion complexes in the carbonyl stretching frequency region are measured by mass-selected infrared photodissociation spectroscopy. The six-coordinated $TM(CO)_6^-$ anions are determined to be the coordination saturate complexes for both the group IV and group V metals. The $TM(CO)_6^-$ complexes of group IV metals (TM=Ti, Zr, Hf) are 17-electron complexes having a $^2A_{1g}$ ground state with D_{3d} symmetry, while the $TM(CO)_6^-$ complexes of group V metals (TM=V, Nb, Ta) are 18-electron species with a closed-shell singlet ground state possessing O_h symmetry. The energy decomposition analyses indicate that the metal-CO covalent bonding is dominated by $TM^-(d)\rightarrow(CO)_6$ π-backdonation and $TM^-(d)\leftarrow(CO)_6$ σ-donation interactions.

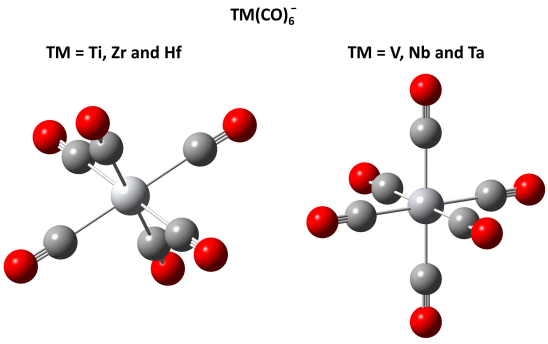

Key words: Infrared photodissociation spectroscopy, Metal carbonyl complex, 18-Electron rule, Molecular structure

I. INTRODUCTION

The electron counting rules are nowadays still widely used to explain the stability of molecules. Transition metal atoms use their ns, np and $(n-1)$d valence atomic orbitals for covalent bonding, and thus obey the 18-electron rule [1]. Homoleptic transition metal carbonyl complexes are archetypical examples for demonstrating the metal-ligand bonding and the 18-electron rule [2]. Mononuclear transition metal carbonyl complexes of groups 10, 8 and 6 such as $Ni(CO)_4$, $Fe(CO)_5$, and $Cr(CO)_6$, are stable homoleptic carbonyls that obey the 18-electron rule. The early transition metals with fewer valence electrons need to bind more carbonyl ligands to accomplish the 18-electron configuration. But high coordination may cause steric repulsion between the ligands. Therefore, the 18-electron rule is considered to be less strict for early transition metals. $V(CO)_6$ is a highly reactive but isolable homoleptic metal carbonyl complex with only 17 valence electrons [3]. Earlier matrix isolation spectroscopic studies also suggest that the 16-electron six-coordinate carbonyl complexes of group IV atoms $TM(CO)_6$ (TM=Ti, Zr, Hf) are formed in solid matrices [4–6] rather than the seven-coordinate 18-electron $TM(CO)_7$ complexes which are theoretically predicted to be stable species [7].

The seven-coordinate homoleptic carbonyl cation $Ti(CO)_7^+$ was produced and determined to have a bond dissociation energy of 0.54±0.07 eV using guided ion beam mass spectrometry in the gas phase [8]. But later infrared photodissociation spectroscopic studies

*Authors to whom correspondence should be addressed. E-mail: gjwang@fudan.edu.cn, mfzhou@fudan.edu.cn

 ©2022 Chinese Physical Society

revealed that the 15-electron $TM(CO)_6^+$ rather than the 17-electron $TM(CO)_7^+$ complexes are the fully coordinated complexes for TM=Ti, Zr, Hf [9, 10]. In the cases of group III and group V metals, the heavier metal cations form the expected 18-electron complexes $TM(CO)_7^+$ (TM=Nb, Ta) and $TM(CO)_8^+$ (TM=Y, La), but the lighter Sc^+ and V^+ ions form only the 16-electron complexes $Sc(CO)_7^+$ and $V(CO)_6^+$ [11–14]. Very recently, the 18-electron $Nb(CO)_7^+$ and $Ta(CO)_7^+$ cations were isolated as stable salt compounds [15].

We found that the group III elements scandium, yttrium and lanthanum can bind eight CO ligands to form the octa-coordinate anion complexes $TM(CO)_8^-$ (TM=Sc, Y, La) in the gas phase [16]. The octacarbonyl neutral complexes $TM(CO)_8$ for TM=Zr, Hf, which are isoelectronic with the group III anion complexes are also formed in solid noble gas matrices [17]. In the case of Ti, only the heptacarbonyl $Ti(CO)_7$ is observed. The octacarbonyl complexes $TM(CO)_8^-$ (TM=Sc, Y, La) and $TM(CO)_8$ (TM=Zr, Hf) are formally 20-electron species, which possess cubic (O_h) symmetry. Bonding analyses indicate that one (a_{2u}) occupied valence molecular orbital (MO) of the complexes having cubic (O_h) symmetry has only coefficients at the CO ligands. The valence atomic orbitals of the metals do not have proper symmetry to mix with the a_{2u} MO of $(CO)_8$. These 20-electron complexes thus still obey the 18-electron rule if only those valence electrons bind to the metal are counted. By using a Smalley-type laser vaporization/supersonic-expansion ion source involving a growth channel, the 19-electron octacarbonyl cation complexes of zirconium and hafnium are also formed in the gas phase [17].

In this report, we extend our studies to the coordinatively saturated carbonyl anion complexes of group IV and group V metals $TM(CO)_{6,7}^-$. A combined infrared spectroscopic and theoretical study confirm that both group IV and group V metals form only six-coordinated $TM(CO)_6^-$ anion complexes in the gas phase.

II. EXPERIMENTAL AND THEORETICAL METHOD

The infrared photodissociation spectroscopic experiments are performed using a collinear tandem time-of-flight mass spectrometer (TOF-MS) coupled with a pulsed laser vaporation-supersonic expansion ion source, as described in detail previously [18]. Briefly, the $TM(CO)_n^-$ anions are produced using a Smalley-type laser vaporization supersonic expansion ion source. The 1064 nm fundamental of a pulsed Nd:YAG laser (Continuum, Minilite II, 10 Hz repetition rate) is used to ablate a translating metal target. The anion complexes are produced from the laser vaporization process in expansions of helium seeded with 10% CO using a pulsed valve (General Valve, Series 9) at 0.6−1.0 MPa backing pressure. The ion beam after supersonic expansion is skimmed and mass separated by a time-of-flight mass spectrometer. The anions of interest are mass-selected, decelerated, and subjected to infrared photodissociation by a tunable infrared laser beam provided by an OPO/OPA system (Laser Vision) pumped by a Nd:YAG laser (Continuum, Surelite EX). The fragment anions together with the undissociated parent anions are reaccelerated and detected by a second collinear time-of-flight mass spectrometer. IR spectra are recorded by monitoring the relative yield of fragment anions as a function of the photodissociation IR laser wavelength. The wavenumber of the infrared beam is calibrated using the absorption spectrum of carbon monoxide gas with an error of less than 2.0 cm^{-1}.

Density functional theory (DFT) calculations are performed in order to determine the structures of the $TM(CO)_n^-$ (n=6, 7) complexes. Calculations are performed with the B3LYP functional [19, 20] using the Gaussian 09 computational package [21]. Dispersion corrections are considered by using Grimme's coefficients [22]. The Def2-TZVPP [23, 24] basis set is used for all atoms and quasi-relativistic effective core potentials are used for the Zr, Hf, Nb, and Ta atoms. The computed harmonic vibrational frequencies are scaled by a factor of 0.968 and given an 8 cm^{-1} FWHM Lorentzian line shape comparied to the experimental spectra.

III. RESULTS AND DISCUSSION

FIG. 1 displays the typical mass spectra of carbonyl anion complexes of Ti and V. The mass spectra from other groups IV and V metals are shown in FIG. S1 and FIG. S2 of Supplementary materials (SM). Each spectrum exhibits a progression of mononuclear carbonyl complexes $TM(CO)_n^-$ (TM=Ti, Zr, Hf, V, Nb, Ta, n=2−7). Peaks of $TM(CO)_n^-$ are also presented with appreciable intensities for some metals such as hafnium. In each spectrum, the $TM(CO)_6^-$ anion is the most intense peak, the peak intensity decreases dramatically from n=6 to 7. These observations indicate that the

DOI:10.1063/1674-0068/cjcp2105096 ©2022 Chinese Physical Society

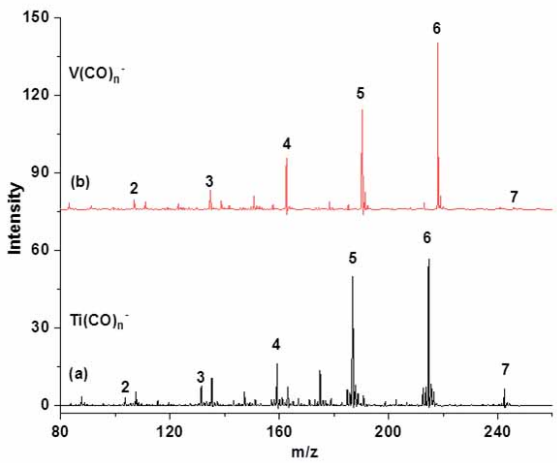

FIG. 1 Mass spectra of the metal carbonyl anion complexes produced by pulsed laser vaporization of metal target in an expansion of helium seeded by carbon monoxide. (a) $Ti(CO)_n^-$ and (b) $V(CO)_n^-$ (n=2−7).

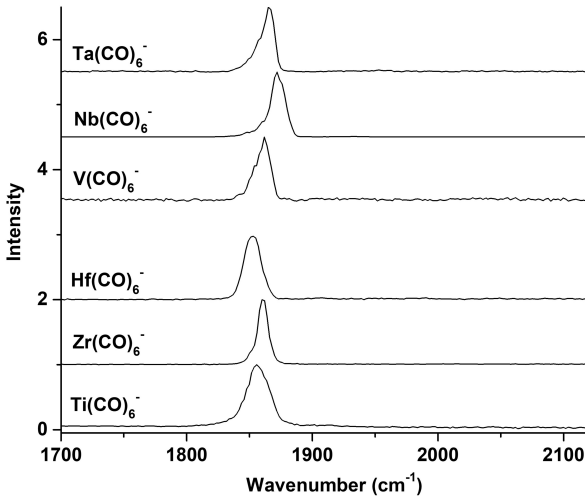

FIG. 2 Infrared photodissociation spectra of $TM(CO)_6^-$ in the 1700−2150 cm^{-1}.

$TM(CO)_6^-$ anions are formed preferentially with high stability, suggesting that they are the coordination saturate complexes.

All the $TM(CO)_6^-$ anions photodissociate by losing a neutral CO fragment when being irradiated by focused infrared laser beam in the carbonyl stretching frequency region with dissociation efficiency ranging from 3% to 15%. The low efficiency with focused laser beam suggests that the photodissociation is a multiple photon process. The sixth CO bond dissociation energy of $V(CO)_6^-$ has been experimentally determined to be 30.8±3.5 kcal/mol by collision-induced-dissociation experiments [25], which is significantly higher than the IR photon energy in the carbonyl stretching frequency region. The infrared photodissociation spectra of $TM(CO)_6^-$ are shown in FIG. 2. The calculated and experimental frequencies are listed in Table I. Each anion has only one band in the carbonyl stretching frequency region. The band positions of the $Ti(CO)_6^-$ and $V(CO)_6^-$ anions at 1856 and 1862 cm^{-1} are slightly red-shifted from the corresponding values of 1861 and 1873 cm^{-1} in solid neon matrix [5]. The infrared spectra of $Na^+TM(CO)_6^-$ (TM=V, Nb, Ta) have been measured in solution [26], exhibiting bands at 1862, 1875, and 1867 cm^{-1}, which are very close to the present gas phase values.

The $TM(CO)_7^-$ anions are also selected for photodissociation. It is found that all the $TM(CO)_7^-$ anions exhibit quite high dissociation efficiency with unfocused infrared laser beam. The dissociation efficiency ranges from 40% to 70%, indicating that the dissociation proceeds via a single photon process and that the seventh CO ligand is weakly bonded. The infrared photodissociation spectra of $TM(CO)_7^-$ are shown in FIG. S3 of SM. The spectra in the 1800−1900 cm^{-1} region are quite similar to those of $TM(CO)_6^-$ except that the band positions are about 10 cm^{-1} blue-shifted from that of $TM(CO)_6^-$. Besides the bands in the 1800−1900 cm^{-1} region, each anion exhibits an additional weak band in the 2130−2140 cm^{-1} region. The band position is very close to that of free CO at 2143 cm^{-1} and can be assigned to the absorption of weakly bound CO ligand [27, 28]. The mass spectral and infrared photodissociation spectral results both point to the conclusion that for both group IV and group V metals, the $TM(CO)_6^-$ anions are the coordination saturate complexes, while the $TM(CO)_7^-$ anions are weakly bound complexes involving a $TM(CO)_6^-$ core anion. Notice for $Zr(CO)_7^-$ the perturbation of the peripheral CO leads to a well-resolved split of the main band.

To gain insight into the geometric and electronic structures and bonding of these anion complexes, theoretical calculations have been performed. The optimized structures for $TM(CO)_6^-$ are displayed in FIG. 3. For each of the $TM(CO)_6^-$ complexes of group IV metals, the most stable structure has a doublet electronic ground state with D_{3d} symmetry. The neutral $TM(CO)_6$ complexes were theoretically predicted to have similar D_{3d} symmetry structures as well [7]. Besides the D_{3d} structure, another isomer with C_{2v} sym-

DOI:10.1063/1674-0068/cjcp2105096 ©2022 Chinese Physical Society

TABLE I Comparison between the experimental and calculated carbonyl stretching vibrational frequencies of the $TM(CO)_6^-$ anion complexes (TM=Ti, Zr, Hf, V, Nb, Ta). The theoretical frequencies are calculated at the B3LYP-D3(BJ)/def2-TZVP/ECP level. The IR intensities are listed in parentheses in km/mol and are scaled by a factor of 0.968.

Complex	Symmetry	Frequency/cm^{-1}	
		Calc.	Expt.
$Ti(CO)_6^-$	D_{3d}	1864 (0, e_g), 1878 (2356, a_{2u}), 1878 (3289×2, e_u), 2003 (0, a_{1g})	1856
$Zr(CO)_6^-$	D_{3d}	1875 (0, e_g), 1878 (2545, a_{2u}), 1883 (3628×2, e_u), 2001 (0, a_{1g})	1861
$Hf(CO)_6^-$	D_{3d}	1869 (0, e_g), 1874 (2643, a_{2u}), 1878 (3643×2, e_u), 2002 (0, a_{1g})	1855
$V(CO)_6^-$	O_h	1882 (2745×3, t_{1u}), 1903 (0, e_g), 2012 (0, a_{1g})	1862
$Nb(CO)_6^-$	O_h	1884 (3030×3, t_{1u}), 1905 (0, e_g), 2017 (0, a_{1g})	1872
$Ta(CO)_6^-$	O_h	1882 (3066×3, t_{1u}), 1902 (0, e_g), 2017 (0, a_{1g})	1866

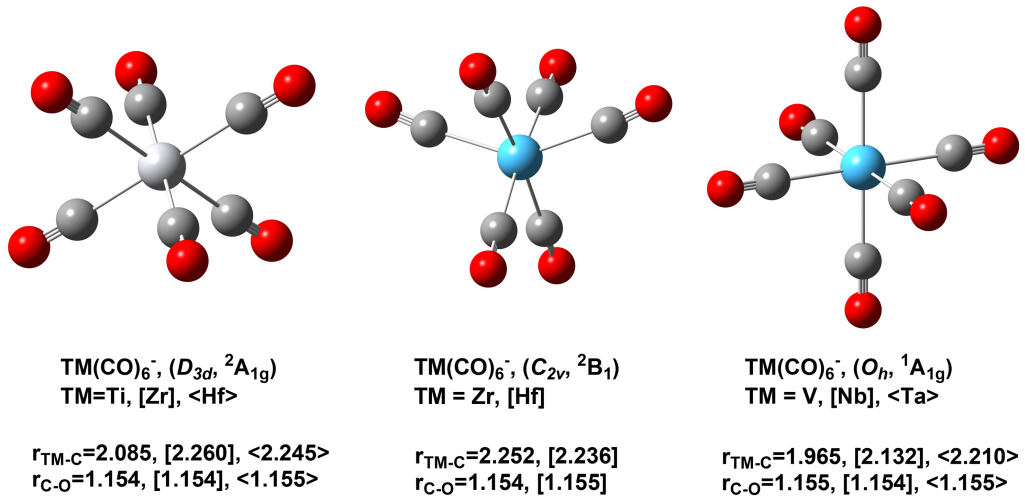

FIG. 3 Optimized structures of the $TM(CO)_6^-$ isomers (TM=Ti, Zr, Hf, V, Nb, Ta). The bond lengths are in Å.

metry is also predicted to be stable structure for both $Zr(CO)_6^-$ and $Hf(CO)_6^-$. This C_{2v} symmetry isomer is predicted to be only 0.3 kcal/mol for $Zr(CO)_6^-$ and 0.2 kcal/mol for $Hf(CO)_6^-$ less stable than the D_{3d} isomer. In the case of hafnium, a third isomer with D_{4h} symmetry is also predicted to be local minimum (FIG. S4 in SM), which lies about 17.2 kcal/mol above the D_{3d} isomer. The calculated carbonyl stretching frequencies scaled by a factor of 0.968 are listed in Table I.

The scaling factor comes from the ratio of the experimental stretching frequency of 2143 cm^{-1} for CO to the calculated value of 2214 cm^{-1} at the B3LYP/ Def2-TZVPP level. Each $TM(CO)_6^-$ anion complex with D_{3d} symmetry has six carbonyl stretching modes, but only three of them are IR active, namely the a_{2u} mode and the doubly degenerate e_u modes. For the $Ti(CO)_6^-$ anion, the a_{2u} and e_u modes are predicted to absorb at the same frequency of 1878 cm^{-1}. These two modes are predicted to be separated by only 4 cm^{-1} and 5 cm^{-1} for the $Zr(CO)_6^-$ and $Hf(CO)_6^-$ anions, respectively. The predicted spectra are consistent with the experimental observation that only one band is observed in the carbonyl stretching frequency region for each anion complex (see FIG. S5 in SM). All of the six carbonyl stretching modes of the C_{2v} symmetry structures are IR active, but the most prominent modes are narrow-spaced (Table I). The coexistence of the C_{2v} symmetry isomer cannot be ruled out for Zr and Hf (FIG. S5 in SM).

The structures of $TM(CO)_6^-$ of group V metals have been theoretically predicted previously [29–31]. In agreement with previous calculations, the $TM(CO)_6^-$ (TM=V, Nb, Ta) anion complexes are predicted to have octahedral structures with O_h symmetry and a closed-shell singlet electronic ground state. Each $TM(CO)_6^-$ anion with octahedral O_h symmetry has only one triply degenerate carbonyl stretching mode that is IR active, which is predicted to be at 1882, 1884, and 1882 cm^{-1}

DOI:10.1063/1674-0068/cjcp2105096 ©2022 Chinese Physical Society

for TM=V, Nb and Ta, respectively, very close to the experimental values (FIG. S6 in SM).

Considering that the octa-coordinated carbonyl anion complexes of group III metals $TM(CO)_8^-$ (TM=Sc, Y, La) and the octa-coordinated carbonyl neutral complexes of Zr and Hf were characterized to be formed in the gas phase or in solid noble gas matrix [16, 17], all of which are formally 20-valence electron species, one would expect that the seven-coordinated anion complexes of group IV and group V metals with 19- and 20-valence electrons might also be viable. As mentioned above, the infrared photodissociation spectroscopic investigations on $TM(CO)_7^-$ confirm that the seven-coordinate complexes are not formed in the gas phase, and that the observed anion species are due to weakly bound CO-tagged complexes involving a $TM(CO)_6^-$ anion core. Geometry optimizations on various possible structures of $TM(CO)_7^-$ (TM=Zr, Hf, V, Nb, Ta) converge to the CO-tagged structures and fail to locate any minimum structure with seven-coordination. A seven-coordinate isomer with a C_{3v} symmetry structure is predicted for the $Ti(CO)_7^-$ anion, which is less stable than the CO-tagged isomer by 3.2 kcal/mol (FIG. S7 in SM).

The bonding of the $TM(CO)_6^-$ anion complexes of group V metals is simplified by the high symmetry of the structures. FIG. 4(a) shows the orbital correlation diagram between the valence orbitals of a group V metal anion in the cubic (O_h) field of six CO ligands and the 5σ and $2\pi^*$ valence MOs of $(CO)_6$. The $(n-1)$d orbitals of metal split into two irreducible representations of the O_h point group, namely, the doubly degenerate e_g atomic orbitals (AOs) and the triply degenerate t_{2g} AOs. Following the Dewar-Chatt-Duncanson bonding model [32, 33], the occupied 5σ MOs of $(CO)_6$ donate electronic charge into the vacant ns (a_{1g}), $(n-1)$d (e_g), and np (t_{1u}) AOs of the metal, and the occupied metal $(n-1)$d (t_{2g}) AOs back donate d_π electrons into the vacant $2\pi^*(t_{2g})$ MOs of $(CO)_6$. The orbital interactions of the metal and the ligands give valence molecular orbitals that have a_{1g}, t_{1u}, e_g, and t_{2g} symmetry in the order of increasing energy. The atomic reference configurations for the singlet state of group V metal anions are $(n-1)d^6ns^0np^0$. FIG. 4(b) shows the orbital correlation diagram between the metal valence AOs and six CO ligands for the group IV metal anion complexes $TM(CO)_6^-$ (TM=Ti, Zr, Hf) by using the D_{3d} symmetry of the equilibrium structures. It looks slightly more complicated than the MO diagram for the O_h field of the

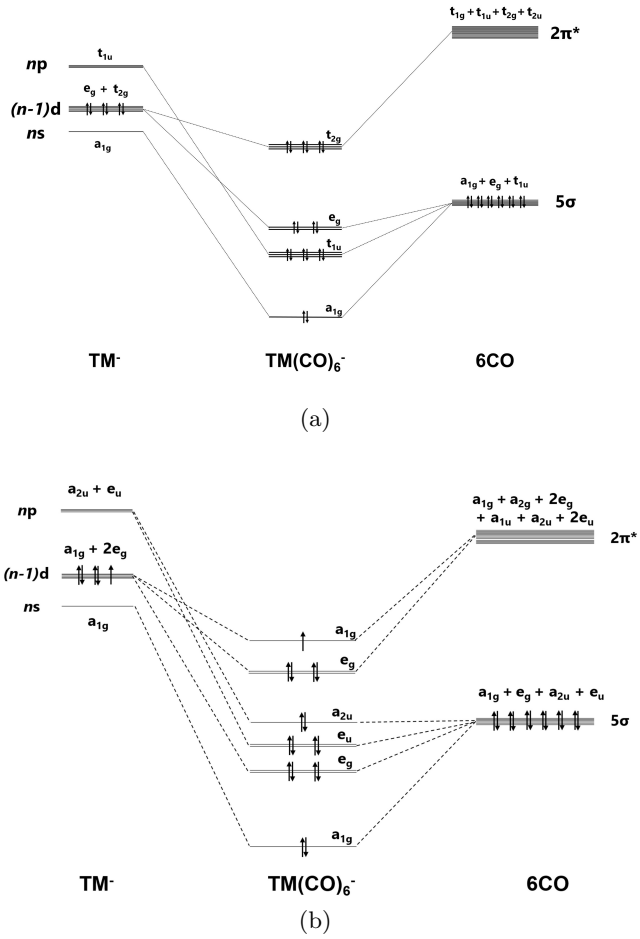

FIG. 4 Correlation diagram of the splitting of the valence orbitals of the metals TM^- and the $(CO)_6$ ligands in the carbonyl anion complexes $TM(CO)_6^-$. (a) TM=V, Nb, Ta (O_h), (b) TM=Ti, Zr, Hf (D_{3d}).

group V anion complexes, but the splittings are related to each other. The triply degenerate t_{2g} orbitals of the O_h field split into doubly degenerate e_g orbitals and one non-degenerate a_{1g} orbital. The t_{1u} orbitals split into e_u and a_{2u}. The orbital correlation diagram suggests that the atomic reference configurations for the doublet state of group IV metal anions are $(n-1)d^5ns^0np^0$.

The nature of the metal-CO bonds and quantitative information about the strength of the $TM^- \leftarrow (CO)_6$ σ-donation and $TM^-(d) \rightarrow (CO)_6$ π-backdonation can be estimated by the EDA-NOCV (energy decomposition analysis in combination with natural orbitals for chemical valence) method [34]. The numerical EDA-NOCV results of the $TM(CO)_6^-$ anion complexes of groups IV and V metals are shown in Tables II and III, respectively. The strength of the interaction energy ΔE_{int} of the three metals in the same group shows the usual

DOI:10.1063/1674-0068/cjcp2105096 ©2022 Chinese Physical Society

TABLE II The EDA-NOCV results of the O_h symmetric $TM(CO)_6^-$ (TM=V, Nb, Ta) complexes at the PBE/TZ2P//B3LYP-D3/def2-TZVP level. The interacting fragments are the metal anion TM^- in the singlet (S) excited state with a $ns^0np^0(n-1)d^6$ valence electron configuration and $(CO)_6$ in the singlet state. Energy values are given in kcal/mol.

Energy terms	Assignment	$V^-(S)+(CO)_6(S)$	$Nb^-(S)+(CO)_6(S)$	$Ta^-(S)+(CO)_6(S)$
ΔE_{int}		−568.0	−456.6	−523.8
ΔE_{pauli}		308.1	366.3	374.9
ΔE_{elstat} [a]		−324.8 (37.1%)	−329.3 (40.0%)	−376.1 (41.8%)
ΔE_{orb} [a]		−551.3 (62.9%)	−493.6 (60.0%)	−522.6 (58.2%)
$\Delta E_{orb(1)}$ [b,c] (t_{2g})	$[TM(d)]^-\rightarrow(CO)_6$ π back-donation	−487.3 (88.0%)	−370.3 (75.0%)	−383.4 (73.4%)
$\Delta E_{orb(2)}$ [b,d] (e_g)	$[TM(d)]^-\leftarrow(CO)_6$ σ donation	−63.5 (11.5%)	−102.6 (20.8%)	−108.7 (20.8%)
$\Delta E_{orb(3)}$ [b,c] (t_{1u})	$[TM(p)]^-\leftarrow(CO)_6$ σ donation	1.1 (0.0%)	−9.3 (1.9%)	−11.2 (2.1%)
$\Delta E_{orb(4)}$ [b] (a_{1g})	$[TM(s)]^-\leftarrow(CO)_6$ σ donation	1.1 (0.0%)	−3.8 (0.8%)	−9.4 (1.8%)
$\Delta E_{orb(rest)}$ [b]		−2.7 (0.5%)	−7.6 (1.5%)	−9.9 (1.9%)

[a] The values in the parentheses show the contribution to the total attractive interaction $\Delta E_{elstat}+\Delta E_{orb}$.
[b] The values in the parentheses show the contribution to the total orbital interaction $\Delta E_{orb}=\Delta E_{orb(1)}+\Delta E_{orb(2)}+\Delta E_{orb(3)}+\Delta E_{orb(4)}+\Delta E_{orb(rest)}$.
[c] The sum of the three components is given for t_{2g} orbital and t_{1u} orbital, respectively.
[d] The sum of the two components is given for e_g orbital.

TABLE III The EDA-NOCV results of the D_{3d} symmetric $TM(CO)_6^-$ (TM=Ti, Zr, Hf) complexes at the PBE/TZ2P//B3LYP-D3/def2-TZVP level. The interacting fragments are the metal anion TM^- in the doublet (D) excited state with a $ns^0np^0(n-1)d^5$ valence electron configuration and $(CO)_6$ in the singlet state. Energy values are given in kcal/mol.

Energy terms	Assignment	$Ti^-(D)+(CO)_6(S)$	$Zr^-(D)+(CO)_6(S)$	$Hf^-(D)+(CO)_6(S)$
ΔE_{int}		−492.2	−387.6	−448.1
ΔE_{pauli}		243.1	280.0	292.0
ΔE_{elstat} [a]		−258.0 (35.1%)	−260.2 (39.0%)	−289.8 (39.2%)
ΔE_{orb} [a]		−477.3 (64.9%)	−407.4 (61.0%)	−450.3 (60.8%)
$\Delta E_{orb(1)}$ [b,c] (e_g)	$[TM(d)]^-\rightarrow(CO)_6$ π back-donation	−337.6 (70.7%)	−254.2 (62.4%)	−269.0 (59.7%)
$\Delta E_{orb(2)}$ [b] (a_{1g})	$[TM(d)]^-\rightarrow(CO)_6$ π back-donation	−80.2 (16.8%)	−60.5 (14.8%)	−64.8 (14.4%)
$\Delta E_{orb(3)}$ [b,c] (e_g)	$[TM(d)]^-\leftarrow(CO)_6$ σ donation	−47.6 (10.0%)	−68.8 (16.9%)	−76.3 (16.9%)
$\Delta E_{orb(4)}$ [b] (a_{1g})	$[TM(s)]^-\leftarrow(CO)_6$ σ donation	−1.6 (0.3%)	−4.2 (1.0%)	−10.2 (2.3%)
$\Delta E_{orb(5)}$ [b] (a_{2u})	$[TM(p)]^-\leftarrow(CO)_6$ σ donation	−0.1 (0.0%)	−2.7 (0.7%)	−3.6 (0.8%)
$\Delta E_{orb(6)}$ [b,c] (e_u)	$[TM(p)]^-\leftarrow(CO)_6$ σ donation	0.2 (0.0%)	−3.6 (0.9%)	−6.3 (1.4%)
$\Delta E_{orb(rest)}$ [b]		−10.4 (2.2%)	−13.4 (3.3%)	−20.1 (4.5%)

[a] The values in parentheses show the contribution to the total attractive interaction $\Delta E_{elstat}+\Delta E_{orb}$.
[b] The values in parentheses show the contribution to the total orbital interaction $\Delta E_{orb}=\Delta E_{orb(1)}+\Delta E_{orb(2)}+\Delta E_{orb(3)}+\Delta E_{orb(4)}+\Delta E_{orb(5)}+\Delta E_{orb(6)}+\Delta E_{orb(rest)}$.
[c] The sum of the two components is given for e_g or e_u orbital.

V-shaped trend in which the second transition-metal-row metals exhibit the weakest interactions. Note that the strength of interaction of group V metal is slightly stronger than that of the group IV metal in the same row as expected, due to the fact that the group V metals have one more electron available for bonding. The breakdown of the orbital term ΔE_{orb} into the pairwise orbital interactions shows that the major contribution comes from the $TM^-(d)\rightarrow(CO)_6$ π back-donation followed by $TM^-(d)\leftarrow(CO)_6$ σ donation (Tables II and III). The two orbital terms afford >90% of the covalent TM^--$(CO)_6$ bonding. The ns and np valence AOs of metal play a very minor role in the bonding. The EDA-NOCV results indicate that the most important valence orbitals of the metal atoms for the covalent bonds are the $(n-1)$d AOs. The deformation densities

DOI:10.1063/1674-0068/cjcp2105096 ©2022 Chinese Physical Society

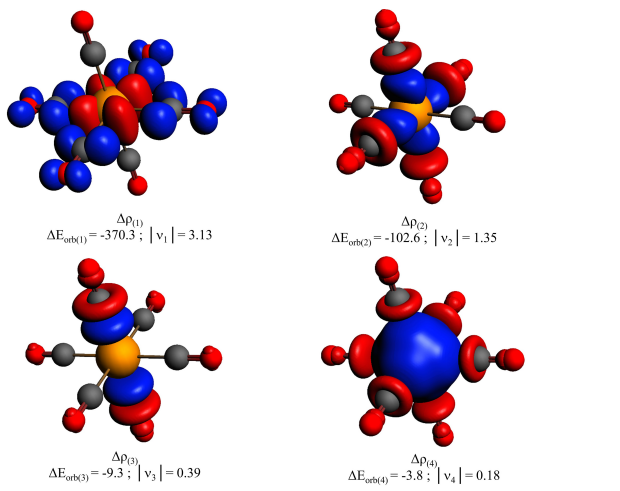

FIG. 5 Plot of the deformation densities $\Delta\rho_{(1)}$, $\Delta\rho_{(2)}$, $\Delta\rho_{(3)}$, and $\Delta\rho_{(4)}$ of $Nb(CO)_6^-$, which are associated with the orbital interactions $\Delta E_{orb(1)}$, $\Delta E_{orb(2)}$, $\Delta E_{orb(3)}$, $\Delta E_{orb(4)}$ in $Nb(CO)_6^-$. The isosurface values are 0.003 a.u. for $\Delta\rho_{(1)}$ and $\Delta\rho_{(1)}$, and 0.001 a.u. for $\Delta\rho_{(3)}$ and $\Delta\rho_{(4)}$. The eigenvalues $|\nu_n|$ give the size of the charge migration in e. The charge flow of the deformation densities is red→blue.

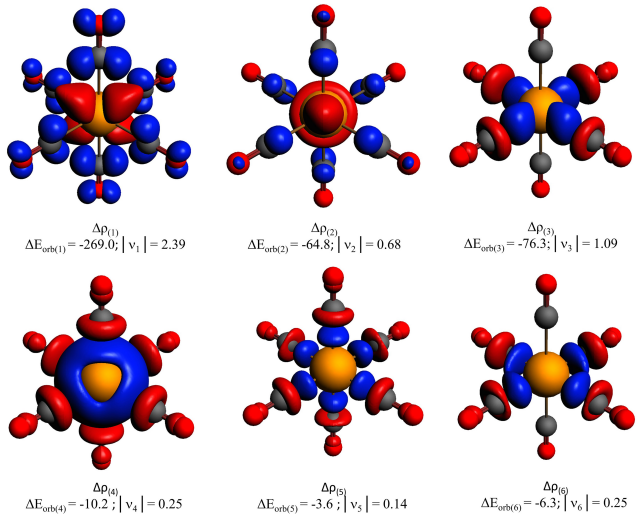

FIG. 6 Plot of the deformation densities $\Delta\rho_{(1)}$, $\Delta\rho_{(2)}$, $\Delta\rho_{(3)}$, $\Delta\rho_{(4)}$, $\Delta\rho_{(5)}$, and $\Delta\rho_{(6)}$ of $Hf(CO)_6^-$, which are associated with the orbital interactions $\Delta E_{orb(1)}$, $\Delta E_{orb(2)}$, $\Delta E_{orb(3)}$, $\Delta E_{orb(4)}$, $\Delta E_{orb(5)}$, $\Delta E_{orb(6)}$ in $Hf(CO)_6^-$. The isosurface values are 0.003 a.u. for $\Delta\rho_{(1)}$, $\Delta\rho_{(2)}$, $\Delta\rho_{(3)}$, and 0.001 a.u. for $\Delta\rho_{(4)}$, $\Delta\rho_{(5)}$, and $\Delta\rho_{(6)}$. The eigenvalues $|\nu_n|$ give the size of the charge migration in e. The charge flow of the deformation densities is red→blue.

$\Delta\rho_{(1)-(4)}$ of $Nb(CO)_6^-$, which are associated with the most important pairwise orbital interactions $\Delta E_{orb(1)}$, $\Delta E_{orb(2)}$, $\Delta E_{orb(3)}$, and $\Delta E_{orb(4)}$ given in Table II are shown in FIG. 5. The deformation densities $\Delta\rho_{(1)}$, $\Delta\rho_{(2)}$, $\Delta\rho_{(3)}$, $\Delta\rho_{(4)}$, $\Delta\rho_{(5)}$, and $\Delta\rho_{(6)}$ of $Hf(CO)_6^-$ are shown in FIG. 6. The color code of the charge migration is red→blue. Only one component of the degenerate orbital interactions is shown. The plots nicely illustrate the charge flow that accompanies the orbital interactions.

IV. CONCLUSION

Mononuclear carbonyl anion complexes of group IV and group V metals $TM(CO)_{6,7}^-$ (TM=Ti, Zr, Hf, V, Nb, Ta) are generated in the gas phase. The mass spectrometric and infrared photodissociation spectroscopic studies indicate that the six-coordinated $TM(CO)_6^-$ anions are the coordination saturate complexes for both the group IV and group V metals. The $TM(CO)_6^-$ complexes of group IV metals (TM=Ti, Zr, Hf) are 17-electron complexes having a $^2A_{1g}$ ground state with D_{3d} symmetry, while the $TM(CO)_6^-$ complexes of group V metals (TM=V, Nb, Ta) are 18-electron species with a closed-shell singlet ground state possessing O_h symmetry. The energy decomposition analyses indicate that the metal-CO covalent bonding are dominated by $TM^-(d)\rightarrow(CO)_6$ π-backdonation and $TM^-(d)\leftarrow(CO)_6$ σ-donation interactions. The $(n-1)$d AOs are the most important valence orbitals of metal for the covalent bonding with the CO ligands.

Supplementary materials: Mass spectra of $TM(CO)_n^-$ (TM=Ti, Zr, Hf, V, Nb, Ta), infrared spectra of $TM(CO)_7^-$, experimental and simulated infrared spectra of $TM(CO)_6^-$, and optimized structures of $Hf(CO)_6^-$ and $Ti(CO)_7^-$ are shown.

V. ACKNOWLEDGMENTS

This work is supported by the National Natural Science Foundation of China (No.21873020 and No.21688102).

[1] I. Langmuir, Science **54**, 59 (1921).
[2] G. Frenking and N. Fröhlich, Chem. Rev. **100**, 717 (2000).
[3] R. Ercoli, F. Calderazzo, and A. Alberola, J. Am. Chem. Soc. **82**, 2966 (1960).
[4] R. Busby, W. Klotzbucher, and G. A. Ozin, Inorg. Chem. **16**, 822 (1977).
[5] M. F. Zhou and L. Andrews, J. Phys. Chem. A **103**, 5259 (1999).
[6] M. F. Zhou and L. Andrews, J. Am. Chem. Soc. **122**, 1531 (2000).

DOI:10.1063/1674-0068/cjcp2105096 ©2022 Chinese Physical Society

[7] Q. Luo, Q. S. Li, Z. H. Yu, Y. Xie, R. B. King, and H. F. Schaefer, J. Am. Chem. Soc. **130**, 7756 (2008).
[8] F. Meyer and P. B. Armentrout, Mol. Phys. **88**, 187 (1996).
[9] A. D. Brathwaite and M. A. Duncan, J. Phys. Chem. A **117**, 11695 (2013).
[10] X. J. Zhou, J. M. Cui, Z. H. Li, G. J. Wang, Z. P. Liu, and M. F. Zhou, J. Phys. Chem. A **117**, 1514 (2013).
[11] A. D. Brathwaite, J. A. Maner, and M. A. Duncan, Inorg. Chem. **53**, 1166 (2014).
[12] H. Xie, J. Wang, Z. B. Qin, L. Shi, Z. C. Tang, and X. P. Xing, J. Phys. Chem. A **118**, 9380 (2014).
[13] A. M. Ricks, Z. D. Reed, and M. A. Duncan, J. Am. Chem. Soc. **131**, 9176 (2009).
[14] A. M. Ricks, A. D. Brathwaite, and M. A. Duncan, J. Phys. Chem. A **117**, 1001 (2013).
[15] W. Unkrig, M. Schmitt, D. Kratzert, D. Himmel, and I. Krossing, Nat. Chem. **12**, 647 (2020).
[16] J. Jin, T. Yang, K. Xin, G. Wang, X. Jin, M. Zhou, and G. Frenking, Angew. Chem. Int. Ed. **57**, 6236 (2018).
[17] G. Deng, S. Lei, S. Pan, J. Jin, G. Wang, L. Zhao, M. Zhou, and G. Frenking, Chem. Eur. J. **26**, 10487 (2020).
[18] G. J. Wang, C. X. Chi, X. P. Xing, C. F. Ding, and M. F. Zhou, Sci. China Chem. **53**, 1166 (2014).
[19] C. Lee, W. Yang, and R. G. Parr, Phys. Rev. B **37**, 785 (1988).
[20] A. D. Becke, J. Chem. Phys. **98**, 5648 (1993).
[21] M. J. Frisch, G. W. Trucks, H. B. Schlegel, G. E. Scuseria, M. A. Robb, G. Cheeseman, J. R. Scalmani, V. Barone, B. Mennucci, G. A. Petersson, H. Nakatsuji, M. Caricato, X. Li, H. P. Hratchian, A. F. Izmaylov, J. Bloino, G. Zheng, J. L. Sonnenberg, M. Hada, M. Ehara, K. Toyota, R. Fukuda, J. Hasegawa, M. Ishida, T. Nakajima, Y. Honda, O. Kitao, H. Nakai, T. Vreven, J. A. J. Montgomery, J. E. Peralta, F. Ogliaro, M. Bearpark, J. J. Heyd, E. Brothers, K. N. Kudin, V. N. Staroverov, R. Kobayashi, J. Nomand, K. Raghavachari, A. Rendell, J. C. Burant, S. S. Iyengar, J. Tomasi, M. Cossi, N. Rega, J. M. Millam, M. Klene, J. E. Knox, J. B. Cross, V. Bakken, C. Adamo, J. Jaramillo, R. Gomperts, R. E. Stratmann, O. Yazyev, A. J. Austin, R. Cammi, C. Pomelli, J. W. Ochterski, R. L. Martin, K. Morokuma, V. G. Zakrzewski, G. A. Voth, P. Salvador, J. J. Dannenberg, S. Dapprich, A. D. Daniels, O. Farkas, J. B. Foresman, J. V. Ortiz, J. Cioslowski, and D. J. Fox, *Gaussian 09, Revision A02*, Wallingford CT: Gaussian Inc., (2009).
[22] S. Grimme, J. Antony, S. Ehrlich, and H. Krieg, J. Chem. Phys. **132**, 154104 (2010).
[23] F. Weigend, Phys. Chem. Chem. Phys. **8**, 1057 (2006).
[24] F. Weigend and R. Ahlrichs, Phys. Chem. Chem. Phys. **7**, 3297 (2005).
[25] L. S. Sunderlin, D. Wang, and R. R. Squires, J. Am. Chem. Soc. **115**, 12060 (1993).
[26] F. Calderazzo, U. Englert, G. Pampaloni, G. Pelizzi, and R. Zamboni, Inorg. Chem. **22**, 1865 (1983).
[27] G. J. Wang, C. X. Chi, J. M. Cui, X. P. Xing, and M. F. Zhou, J. Phys. Chem. A **116**, 2484 (2012).
[28] C. X. Chi, H. Qu, L. Y. Meng, F. C. Kong, M. B. Luo, and M. F. Zhou, Angew. Chem. Int. Ed. **56**, 14096 (2017).
[29] V. Jonas and W. Thiel, Organometallics **17**, 353 (1998).
[30] R. K. Szilagyi and G. Frenking, Organometallics **16**, 4807 (1997).
[31] A. Diefenbach, F. M. Bickelhaupt, and G. Frenking, J. Am. Chem. Soc. **122**, 6449 (2000).
[32] M. J. S. Dewar, Bull. Soc. Chim. Fr. **18**, C79 (1951).
[33] J. Chatt and L. A. Duncanson, J. Chem. Soc. 2939 (1953).
[34] M. P. Mitoraj, A. Michalak, and T. Ziegler, J. Chem. Theory Comput. **5**, 962 (2009).

DOI:10.1063/1674-0068/cjcp2105096 ©2022 Chinese Physical Society